BIOCHEMISTRY
including biophysical chemistry & molecular biology

Article

pubs.acs.org/biochemistry

TrpB2 Enzymes are *O*-Phospho-L-serine Dependent Tryptophan Synthases

Florian Busch,[‡] Chitra Rajendran,[‡] Olga Mayans,[†] Patrick Löffler,[‡] Rainer Merkl,[‡] and Reinhard Sterner*[,‡]

[‡]Institute of Biophysics and Physical Biochemistry, University of Regensburg, Universitätsstrasse 31, D-93053 Regensburg, Germany
[†]Institute of Integrative Biology, University of Liverpool, Crown Street, Liverpool L69 7ZB, United Kingdom

Supporting Information

ABSTRACT: The rapid increase of the number of sequenced genomes asks for the functional annotation of the encoded enzymes. We used a combined computational−structural approach to determine the function of the TrpB2 subgroup of the tryptophan synthase β chain/β chain-like TrpB1−TrpB2 family (IPR023026). The results showed that TrpB2 enzymes are *O*-phospho-L-serine dependent tryptophan synthases, whereas TrpB1 enzymes catalyze the L-serine dependent synthesis of tryptophan. We found a single residue being responsible for the different substrate specificities of TrpB1 and TrpB2 and confirmed this finding by mutagenesis studies and crystallographic analysis of a TrpB2 enzyme with bound *O*-phospho-L-serine.

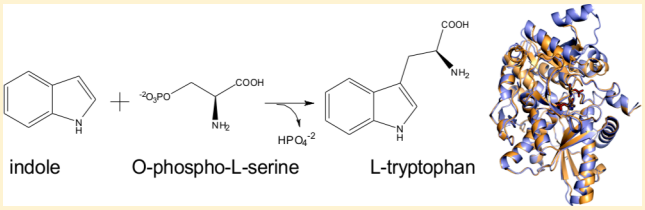

The tryptophan synthase β chain/β chain-like family (IPR023026) consists of two distinct groups, TrpB1 and TrpB2, which share a sequence identity of approximately 30%.[1,2] Dimeric TrpB1 associates with two monomeric α-subunits, TrpA, to the heterotetrameric $\alpha\beta\beta\alpha$ tryptophan synthase complex in which the two different kinds of subunits stimulate each other.[3,4] The TrpA reaction generates glyceraldehyde-3-phosphate and indole. The latter is channeled to the active site of TrpB1 where it reacts with L-serine to form tryptophan in a PLP-dependent condensation reaction.[5−7] Both TrpB1 and TrpA are encoded within the *trp* operon.

The TrpB2 group can be further subdivided into TrpB2i, which is encoded within the *trp* operon, and TrpB2a and TrpB2o, which are encoded outside the *trp* operon.[1] It has been shown that the ssTrpB2i enzyme from *Sulfolobus solfataricus* forms with ssTrpA a transient, ligand-dependent tryptophan synthase complex having $\alpha\beta\beta$ stoichiometry.[8,9] This finding indicates a functional equivalence of TrpB2i and TrpB1 *in vivo*. In contrast, all TrpB2o and TrpB2a enzymes characterized to date do not interact with TrpA.[10,11] Nonetheless, *in vitro* they catalyze the PLP-dependent synthesis of L-tryptophan with a K_m for indole in the nanomolar range and a K_m for L-serine in the high millimolar range. However, the intracellular concentration of L-serine is supposed to be far below this K_m value,[12] suggesting that TrpB2 uses a different substrate for tryptophan biosynthesis *in vivo*. For this reason, we have investigated the substrate specificity of TrpB2 based on structural considerations.

MATERIALS AND METHODS

Cloning. st*trp*B1 was amplified from pBR322-st*trp*AB (a gift from Dr. Ilme Schlichting) using the oligonucleotides AGC CAT ATG ACA ACA CTT CTC AAC CCC TAC and CTG GTG CAA GCT TGA TTT CCC CTC GCG CTT TCA GGA TATC and inserted into pET24a(+) at the *Nde*I/*Hin*dIII restriction sites. tm*trp*B2o was amplified from pET21a(+)-tm*trp*B2o[10] using the oligonucleotides ACC GCA TAT GAG AAT TGT TGT GAA and CCC AGG AAT TCA GGC TTT CAC ACG TAC GCT GT and inserted into pET28a(+) at the *Nde*I/ *Hin*dIII restriction sites. at*trp*B2o was amplified from cDNA of *Arabidopsis thaliana* Col-0 using the oligonucleotides GCA GCT TTG AGA TCT ACT CA and TTA TGG GGC CAT TCG AGC TT. The amplification product was the template in a second round of PCR using the oligonucleotides CTA GCT TAA GAC ATA TGG CAG CTT TGA GA and TTA TGG GGC CAT GGA TCC TTA AAC AAC A. The final amplification product was inserted into the pET28a(+) expression vector at the *Nde*I/ *Bam*HI restriction sites. ss*trp*B2a was amplified from pET28a(+)-ss*trp*B2a[9] using the oligonucleotides TAA TAC GAC TCA CTA TAG GG and CCG CAA GCT TCT CCT TAA ATA ACA C and inserted into pET24a(+) at the *Nde*I/ *Hin*dIII restriction sites. ss*trp*B2a-R337D was generated by QuikChange site-directed mutagenesis[13] from pET28a(+)-ss*trp*B2a using the oligonucleotides TAT GCA GGT GGG CTA GAT TAT CAT GGA GTA GCC and GGC TAC TCC ATG ATA ATC TAG CCC ACC TGC ATA. The mutated gene was subcloned into pET24a(+) at the *Nde*I/*Hin*dIII restriction sites.

Gene Expression and Protein Purification. The proteins ssTrpB2i, ssTrpB2a, ssTrpB2a-R337D and tmTrpB2o were

Received: August 6, 2014
Revised: September 2, 2014
Published: September 3, 2014

   dx.doi.org/10.1021/bi500977y | *Biochemistry* 2014, 53, 6078−6083

expressed with a His_6-tag and purified by a heat step and metal chelate affinity chromatography according to refs 9 and 10. For crystallization, ssTrpB2a was further purified by preparative gel filtration chromatography using an ÄKTA-purifier system with a HiLoad Superdex 75 PG column (120 mL, GE Healthcare).

For expression of stTrpB1, *Escherichia coli* T7 Express (NEB) was transformed with pET24a(+)-st*trp*B. The cells were grown at 37 °C in lysogenic broth (LB) with 50 μg/mL kanamycin to OD_{600} = 0.5. Protein expression was induced by addition of 0.5 mM IPTG. After growth overnight at 20 °C, cells were harvested by centrifugation and disrupted by ultrasonication. The His_6-tagged protein was purified by metal chelate affinity chromatography using an ÄKTA-purifier system with a HisTrap FF crude column (5 mL, GE Healthcare). Proteins in 50 mM Tris/HCl, pH 7.5, and 150 mM NaCl were eluted by a linear gradient of imidazole (10−500 mM) and dialyzed against 50 mM Tris/HCl, pH 7.5.

For expression of atTrpB2o, *E. coli* DE3 (NEB) was transformed with pET28a(+)-at*trp*B2o. The cells were grown at 37 °C in lysogenic broth (LB) with 50 μg/mL kanamycin to OD_{600} = 0.5. Protein expression was induced by addition of 0.5 mM IPTG. After growth overnight at 37 °C, cells were harvested by centrifugation and disrupted by ultrasonication. The His_6-tagged protein was purified by metal chelate affinity chromatography using an ÄKTA-purifier system with a HisTrap FF crude column (5 mL, GE Healthcare). Proteins in 50 mM potassium phosphate, pH 7.5, and 300 mM KCl were eluted by a linear gradient of imidazole (10−500 mM) and dialyzed against 50 mM potassium phosphate, pH 7.5.

Crystallization and Structure Determination. Crystallization trials with ssTrpB2a were performed with the vapor diffusion method in 24 well plates (Quiagen) at 18 °C based on previously established conditions (O. Mayans, unpublished data). Drops contained 1 μL of ssTrpB2a (12.5 mg/mL) in 10 mM 4-(2-hydroxyethyl)-1-piperazineethanesulfonic acid (HEPES), pH 7.5, and 25 mM NaCl and 1 μL of reservoir solution. Equilibration was done against 500 μL of reservoir solution. First crystals appeared after 1 week at 18 °C with 25% PEG-4000, 0.1 M Tris/HCl, pH 7.0, and 100 mM NaCl as reservoir solution. Initially crystals appeared as clusters and were multicrystals. Seeding was tried to produce bigger single crystals with 20−25% PEG-4000, 0.1 M Tris/HCl, pH 7.0/7.5/8.0/8.5, and 100 mM NaCl as reservoir solution. After 1 month at 18 °C, single crystals were collected, soaked with 200 mM *O*-phospho-L-serine, and flash frozen in liquid nitrogen. Data of single crystals were collected at SLS beamline PXIII at 100 K. Data were processed using XDS,[14] and the data quality assessment was done using phenix.xtriage.[15] Molecular replacement was performed with MOLREP within the CCP4i suite.[16] A homology model with ssTrpB2a (O. Mayans, unpublished data) was built with MODELER[17] and served as a search model. Initial refinement was performed using REFMAC.[18] The model was further improved in several refinement rounds using automated restrained refinement with the program PHENIX[15] and interactive modeling with Coot.[19] The final model was analyzed using the program MolProbity.[20]

Substrate Screening. Reaction mixtures (100 μL) contained 100 mM potassium phosphate buffer, pH 7.5, 180 mM KCl,40 μM PLP, 500 μM indole, 2 mM α-amino acid, and 5 μM enzyme. After incubation for 30 min at 25 °C (stTrpB1) or 60 °C (ssTrpB2i, ssTrpB2a, tmTrpB2o, atTrpB2o), reactions were quenched by the addition of 400 μL of methanol. Conversion of indole was subsequently determined by reversed-phase HPLC (Agilent 1200). The separation was performed at 25 °C with a flow rate of 0.25 mL/min on a reversed-phase Gemini-NX-C18 column (3 mm × 150 mm, 3 μm particle size; Phenomenex) using 0.1% formic acid in water as buffer A and 0.1% formic acid in acetonitrile as buffer B. The program was as follows: hold with 5% B for 3 min, linear gradient 5−98% B in 22.8 min, hold with 100% B for 3.6 min, recycle 100−5% B in 3.6 min, and re-equilibrate with 5% B for 12 min. The elution time was 19.7 min for indole.

Kinetic Measurements. Kinetics for the *O*-phospho-L-serine dependent synthesis of tryptophan were measured in 100 mM 3-[4-(2-hydroxyethyl)-1-piperazinyl]propanesulfonic acid (EPPS)/KOH, pH 7.5, 180 mM KCl, and 40 μM PLP with 100 μM indole and varying concentrations of *O*-phospho-L-serine at 80 °C (tmTrpB2o), 60 °C (ssTrpB2a, ssTrpB2i), or 30 °C (atTrpB2o) by absorption spectroscopy using $\Delta\varepsilon_{280}$(tryptophan − indole) = 1.89 mM^{-1} cm^{-1} [21] with a V650 spectrophotometer (d = 1 cm; Jasco).

Fluorescence Titration. Binding of L-serine and *O*-phospho-L-serine to ssTrpB2a and ssTrpB2a-R337D was followed by fluorescence detection at 520 nm after excitation at 440 nm using a FP-6500 spectrofluorometer (d = 1 cm; Jasco). The protein with a subunit concentration of 1 μM was titrated with amino acid at 25 °C in 100 mM potassium phosphate buffer, pH 7.5.

Isothermal Titration Calorimetry (ITC). ITC measurements were performed with a MicroCal iTC200 titration calorimeter (GE healthcare). To this purpose, the proteins were dialyzed against HBS-EP+, 60 mM GP, 10 mM *O*-phospho-L-serine, and 0.05% (w/v) sodium azide. Titrations were conducted at 25 °C by injecting 24 aliquots of 1.6 μL containing 188 μM ssTrpA into 200 μL containing ssTrpB2i at a subunit concentration of 21 μM. The thermodynamic dissociation constant K_d was calculated by a one site binding model implemented in the ITC Origin software.

Surface Plasmon Resonance (SPR). SPR measurements were perfomed on a Biacore X100 optical biosensor (GE healthcare). ssTrpA was covalently immobilized on flow cell 2 of a CM5 sensor chip using EDC/NHS chemistry. The ligand in 10 mM sodium acetate buffer, pH 4.83, was injected to obtain a final signal of 218.2 response units (RU). Interactions were measured at 25 °C at a flow rate of 30 μL/min using various concentrations of ssTrpB2i as analyte in HBS-EP+, 60 mM GP, and 0.05% (w/v) sodium azide in the presence of 10 mM *O*-phospho-L-serine, 1 M L-serine or 1 M glycine. The binding surface was regenerated after each injection with HBS-EP+. K_d values were determined by using a steady-state binding model.

RESULTS AND DISCUSSION

The detailed reaction mechanism of the TrpB2 enzymes is unknown, and no crystal structure has been available for this group so far. In contrast, the structure−function relationship of the TrpB1 group is well understood, mainly based on studies of stTrpB1 from *Salmonella typhimurium*. Here, catalysis involves the formation of an external aldimine between the cofactor PLP and the substrate L-serine. We analyzed the coordination of this intermediate in stTrpB1 and compared it with a most plausible coordination in a homology model generated for ssTrpB2a from *S. solfataricus* (Figure 1).

The cofactor PLP is bound in the same position, and the nitrogen of the pyridinium ring is coordinated by equivalent serine residues in stTrpB1 and ssTrpB2a, which indicates that

dx.doi.org/10.1021/bi500977y | *Biochemistry* 2014, 53, 6078−6083

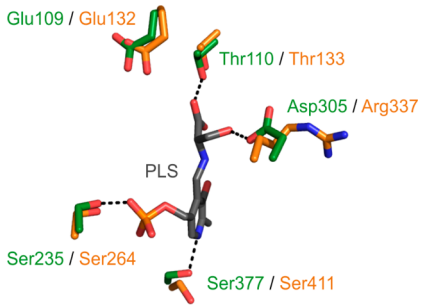

	stTrpB1	ssTrpB2a
binding of cofactor	Ser235	Ser264
cofactor chemistry	Ser377	Ser411
nucleophile specificity	Glu109	Glu132
amine specificity	Thr110	Thr133
	Asp305	Arg337

Figure 1. Superposition of the active sites of stTrpB1 and ssTrpB2a. Active site residues of stTrpB1 (PDB ID 1KFJ) are shown as green sticks and the aldimine between PLP and L-serine (PLS) is shown as gray sticks. Hydrogen bonds between side chains and PLS are indicated by black dashes. ssTrpB2a was modeled by means of Yasara Structure (www.yasara.org) using 1KFJ as template, and superimposed active site residues are shown as yellow sticks. The role of the depicted residues in catalysis is given according to experimental data for stTrpB1.[3,39−43]

both enzyme groups use the same cofactor chemistry. The specificity for using indole as nucleophile is determined by a glutamate residue, which is strictly conserved in all TrpB enzymes. Moreover, both TrpB subfamilies utilize a threonine residue to coordinate the carboxyl moiety of bound L-serine. Whereas the hydroxyl group of L-serine is coordinated by an aspartate in TrpB1, all TrpB2 enzymes have an arginine at that position (Figure S1, Supporting Information). This difference prompted us to test stTrpB1 and various TrpB2 enzymes (ssTrpB2i, ssTrpB2a, tmTrpB2o from *Thermotoga maritima*, and atTrpB2o from *Arabidopsis thaliana*) for their ability to catalyze the conversion of indole with α-amino acids other than L-serine (L-threonine, D-threonine, DL-phenylserine, *O*-phospho-L-threonine, D-serine, L-cysteine, D-cysteine, DL-diaminopropionate, *O*-acetyl-L-serine, *O*-phospho-L-serine, and *O*-phospho-D-serine). The results are shown in Table S1, Supporting Information.

Whereas TrpB1 preferentially uses L-serine as substrate, all studied TrpB2 enzymes have a pronounced preference for *O*-phospho-L-serine. In order to further analyze this finding, we determined the steady-state kinetic parameters of the TrpB2 enzymes for the *O*-phospho-L-serine dependent synthesis of tryptophan and compared them with the parameters of the L-serine dependent synthesis (Table 1).

The $K_m^{\text{O-phospho-L-serine}}$ values of all TrpB2 lie within range of 10−1000 μM, which is found for ∼60% of enzymes in the KEGG database.[22] Since these values are much lower than their $K_m^{\text{L-serine}}$ values and the corresponding turnover numbers k_{cat} are similar, the catalytic efficiencies $k_{cat}/K_m^{\text{O-phospho-L-serine}}$ are higher by about 3−4 orders of magnitude than the catalytic efficiencies $k_{cat}/K_m^{\text{L-serine}}$. We conclude from these results that TrpB2 enzymes catalyze the reaction of indole with *O*-phospho-L-serine *in vivo*. This is a new role for *O*-phospho-L-serine, which has been known up to now only as an intermediate of L-serine, L-cysteine, and L-cystathionine biosynthesis.[23,24]

Table 1. Steady-State Kinetic Parameters of TrpB2 Enzymes with L-Serine and *O*-Phospho-L-serine as Substrates[a]

	k_{cat} (s^{-1})	K_m (mM)	k_{cat}/K_m (M^{-1} s^{-1})
	L-Serine Dependent Reaction		
tmTrpB2o	0.44	50.2	8.7×10^0
ssTrpB2a	0.032	151	2.1×10^{-1}
ssTrpB2i	0.20	35	5.7×10^0
atTrpB2o	0.016	35	4.5×10^{-1}
	O-Phospho-L-serine Dependent Reaction		
tmTrpB2o	0.414	0.316	1.3×10^3
ssTrpB2a	0.015	0.014	1.1×10^3
ssTrpB2i	0.300	0.015	2.0×10^4
atTrpB2o	0.015	0.010	1.5×10^3

[a]Parameters for the L-serine dependent reaction at 80 °C (tmTrpB2o), 60 °C (ssTrpB2a, ssTrpB2i), and 30 °C (atTrpB2o) are according to refs 9, 10, and 44. Conditions for the *O*-phospho-L-serine dependent tryptophan synthase reaction: 100 mM EPPS/KOH, pH 7.5, 180 mM KCl, 40 μM PLP, 100 μM indole. The measurements were made in duplicate with a deviation of less than 30% for the determined constants.

We subsequently solved the structure of the ssTrpB2a dimer with external aldimine between PLP and *O*-phospho-L-serine at one subunit and internal aldimine between PLP and Lys111 at the other subunit (Figure 2; Table S2, Supporting Information). The binding of *O*-phospho-L-serine to the active site of ssTrpB2a leads to a conformational change from an open to a closed state (Figure 2A,B). Such a conformational change upon substrate binding was also observed for stTrpB1.[25,26] As predicted by homology modeling (Figure 1), the cofactor within the active site in the crystal structure is coordinated with hydrogen bonding interactions to Thr133, Ser264, and Ser411 (Figure 2C). Binding of *O*-phospho-L-serine leads to a reorientation of Thr133 and Arg337, which facilitates the coordination of the carbonyl and the phosphate groups of PLP. The replacement of Arg337 by aspartate using site-directed mutagenesis results in the inversion of substrate binding from *O*-phospho-L-serine to L-serine as indicated by fluorescence titration experiments (Table 2).

The closest homologue to tryptophan synthases TrpB1/TrpB2 is the family of cysteine synthases CysM/CysK, which shares the same fold and catalyzes a β-replacement reaction via the same α-aminoacryl intermediate.[27] Recent investigations revealed that some cysteine synthases use *O*-phospho-L-serine instead of *O*-acetyl-L-serine as substrate.[24,28−30] Like in TrpB2 enzymes, the coordination of the phosphate leaving group seems to be accomplished by an arginine residue.[30]

It has been shown that saturating concentrations of the ssTrpA ligand glycerol-3-phosphate (GP) and the ssTrpB2i ligand L-serine induce the formation of a transient $\alpha\beta\beta$ complex.[8] We tested the consequences of replacing L-serine by *O*-phospho-L-serine or glycine for complex formation between ssTrpB2i and ssTrpA. Surface plasmon resonance and isothermal titration calorimetry showed that the affinity between ssTrpB2i and ssTrpA was identical, independent of the used ssTrpB2i ligand (Table S3, Supporting Information). These results indicate that the ssTrpA−ssTrpB2i complex is formed with equal propensity, no matter whether the β-substituent of the ssTrpB2i ligand is −H, $-CH_2OH$, or $-CH_2OPO_3^{2-}$.

dx.doi.org/10.1021/bi500977y | *Biochemistry* 2014, 53, 6078−6083

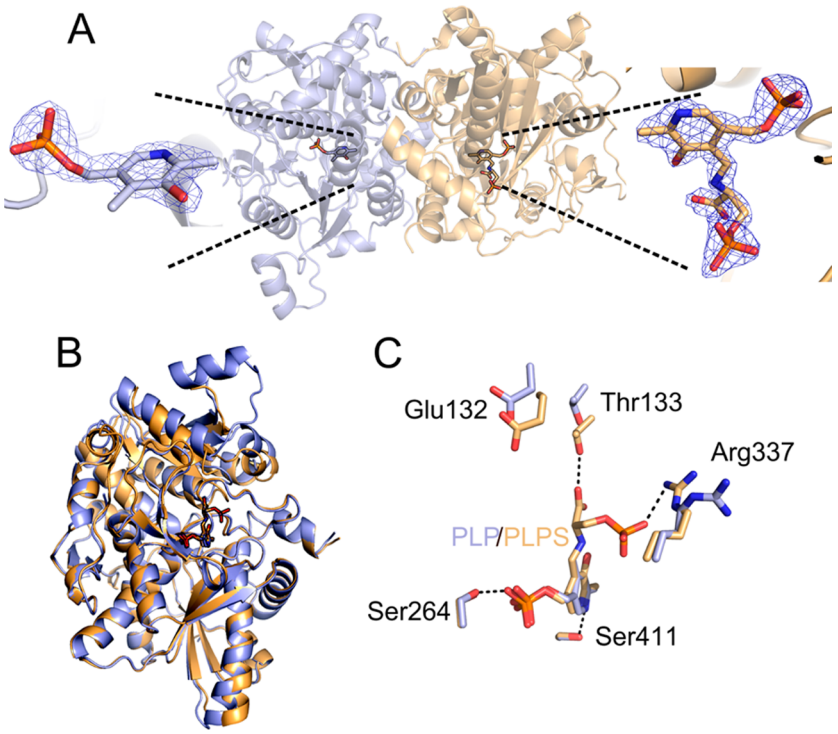

Figure 2. (A) Crystal structure of the ssTrpB2a homodimer (PDB ID 4QYS). The subunit with bound PLP is colored blue; the subunit with the external aldimine between PLP and *O*-phospho-L-serine (PLPS) is colored yellow. Both subunits are shown as ribbon diagrams, and the ligands are shown as sticks. Electron densities for PLP (left panel) and PLPS (right panel) are indicated by a refined $2F_o - F_c$ map, contoured at 0.586 e/Å^3 (2.01 rmsd). (B) Superposition of open and closed conformations of ssTrpB2a. The PLP-bound subunit with open conformation and the PLPS-bound subunit with closed conformation are superimposed. (C) View of the active sites of ssTrpB2a with bound PLP and PLPS. Side chains are shown as balls and sticks, and H-bonds are indicated by black dashes.

Table 2. Binding of L-Serine and *O*-Phospho-L-serine to ssTrpB2a and ssTrpB2a-R337D as Analyzed by Fluorescence Titration[a]

	$K_d^{\text{L-serine}}$ (mM)	$K_d^{\text{O-phospho-L-serine}}$ (mM)
ssTrpB2a wt	*b*	0.08
ssTrpB2a-R337D	4	*b*

[a]Reaction conditions: 100 mM potassium phosphate buffer, pH 7.5. The determined K_d values are shown. The measurements were made in duplicate with a deviation of less than 20% for the determined constants. [b]Undetectably low affinity binding.

The ability of TrpB2 to synthesize tryptophan *in vivo* was recently analyzed using the hyperthermophile *Thermococcus kodakarensis,* which can be genetically manipulated.[31,32] *T. kodakarensis* has a tkTrpB1 enzyme, which is part of the *αββα* tryptophan synthase complex, and a tkTrpB2o enzyme that does not interact with tkTrpA. A *T. kodakarensis* Δ*trp*B1 strain was created, which lacks TrpB1 activity and has an insufficient TrpA activity due to the missing activation by the binding partner. However, Δ*trp*B1 thrived equally well as the wild-type strain in minimal medium supplemented with indole.[11] Also, the transcription of some *trp*B2 genes was shown to be similarly regulated as *trp*B1.[11,33] These findings suggest that TrpB2 enzymes act as tryptophan synthases *in vivo* and primordially evolved for the catalysis of the last step in tryptophan biosynthesis. Interestingly, several organisms harboring TrpB2i or TrpB1 enzymes still possess TrpB2o or TrpB2a proteins. The presence of two TrpB2 enzymes seems to be a minor advantage as indicated by the uneven distribution of TrpB2a in closely related *Sulfolobales* (TrpB2a is present in *S. solfataricus* and *S. tokodaii* but absent in *S. acidocaldarius*). In contrast, differences of TrpB1 and TrpB2 in substrate specificity and affinity may provide a selective advantage by helping to regulate the intracellular concentration of free indole. The specific reason is unclear; however it is known that indole is involved in various biological processes like biofilm formation,[34] cell cycle control,[35,36] and regulation of gene expression.[37,38]

■ ASSOCIATED CONTENT

Supporting Information

Conservation of substrate specifying residue, use of α-amino acids by TrpB enzymes, data collection and refinement statistics, dependence of complex formation between ssTrpA and ssTrpB2i on the TrpB2i ligand, and supporting references. This material is available free of charge via the Internet at http://pubs.acs.org.

Accession Codes

The X-ray coordinates have been deposited in the Protein Data Bank as entry 4QYS.

■ AUTHOR INFORMATION

Corresponding Author

*R.S. Phone: +49-941-943 3015. Fax: +49-941-943 2813. E-mail: Reinhard.Sterner@ur.de.

Notes

The authors declare no competing financial interest.

■ ACKNOWLEDGMENTS

We thank Hermine Reisner and Sonja Fuchs for technical assistance and Vanya Uzunova from GE healthcare for making available the MicroCal iTC200 titration calorimeter.

■ ABBREVIATIONS

at, *Arabidopsis thaliana*; PLP, pyridoxal-5′-phosphate; PLS, aldimine between PLP and L-serine; PLPS, aldimine between PLP and *O*-phospho-L-serine; ss, *Sulfolobus solfataricus*; st, *Salmonella typhimurium*; tk, *Thermococcus kodakarensis*; tm, *Thermotoga maritima*

■ REFERENCES

(1) Merkl, R. (2007) Modelling the evolution of the archeal tryptophan synthase. *BMC Evol. Biol. 7*, 59.
(2) Xie, G., Forst, C., Bonner, C., and Jensen, R. A. (2002) Significance of two distinct types of tryptophan synthase β chain in bacteria, archaea and higher plants. *Genome Biol. 3*, No. RESEARCH0004.
(3) Hyde, C. C., Ahmed, S. A., Padlan, E. A., Miles, E. W., and Davies, D. R. (1988) Three-dimensional structure of the tryptophan synthase $\alpha_2\beta_2$ multienzyme complex from *Salmonella typhimurium*. *J. Biol. Chem. 263*, 17857−17871.
(4) Kirschner, K., Lane, A. N., and Strasser, A. W. (1991) Reciprocal communication between the lyase and synthase active sites of the tryptophan synthase bienzyme complex. *Biochemistry 30*, 472−478.
(5) Huang, X., Holden, H. M., and Raushel, F. M. (2001) Channeling of substrates and intermediates in enzyme-catalyzed reactions. *Annu. Rev. Biochem. 70*, 149−180.
(6) Miles, E. W., Rhee, S., and Davies, D. R. (1999) The molecular basis of substrate channeling. *J. Biol. Chem. 274*, 12193−12196.
(7) Raushel, F. M., Thoden, J. B., and Holden, H. M. (2003) Enzymes with molecular tunnels. *Acc. Chem. Res. 36*, 539−548.
(8) Ehrmann, A., Richter, K., Busch, F., Reimann, J., Albers, S. V., and Sterner, R. (2010) Ligand-induced formation of a transient tryptophan synthase complex with $\alpha\beta\beta$ subunit stoichiometry. *Biochemistry 49*, 10842−10853.
(9) Leopoldseder, S., Hettwer, S., and Sterner, R. (2006) Evolution of multi-enzyme complexes: The case of tryptophan synthase. *Biochemistry 45*, 14111−14119.
(10) Hettwer, S., and Sterner, R. (2002) A novel tryptophan synthase β-subunit from the hyperthermophile *Thermotoga maritima*. Quaternary structure, steady-state kinetics, and putative physiological role. *J. Biol. Chem. 277*, 8194−8201.
(11) Hiyama, T., Sato, T., Imanaka, T., and Atomi, H. (2014) The tryptophan synthase β-subunit paralogs TrpB1 and TrpB2 in *Thermococcus kodakarensis* are both involved in tryptophan biosynthesis and indole salvage. *FEBS J. 281*, 3113−3125.
(12) Bennett, B. D., Kimball, E. H., Gao, M., Osterhout, R., Van Dien, S. J., and Rabinowitz, J. D. (2009) Absolute metabolite concentrations and implied enzyme active site occupancy in *Escherichia coli*. *Nat. Chem. Biol. 5*, 593−599.
(13) Wang, W., and Malcolm, B. A. (1999) Two-stage PCR protocol allowing introduction of multiple mutations, deletions and insertions using QuikChange Site-Directed Mutagenesis. *BioTechniques 26*, 680−682.
(14) Kabsch, W. (2010) Xds. *Acta Crystallogr., Sect. D: Biol. Crystallogr. 66*, 125−132.
(15) Adams, P. D., Grosse-Kunstleve, R. W., Hung, L. W., Ioerger, T. R., McCoy, A. J., Moriarty, N. W., Read, R. J., Sacchettini, J. C., Sauter, N. K., and Terwilliger, T. C. (2002) PHENIX: Building new software for automated crystallographic structure determination. *Acta Crystallogr., Sect. D: Biol. Crystallogr. 58*, 1948−1954.
(16) Potterton, L., McNicholas, S., Krissinel, E., Gruber, J., Cowtan, K., Emsley, P., Murshudov, G. N., Cohen, S., Perrakis, A., and Noble, M. (2004) Developments in the CCP4 molecular-graphics project. *Acta Crystallogr., Sect. D: Biol. Crystallogr. 60*, 2288−2294.
(17) Sali, A., and Blundell, T. L. (1993) Comparative protein modelling by satisfaction of spatial restraints. *J. Mol. Biol. 234*, 779−815.
(18) Murshudov, G. N., Vagin, A. A., and Dodson, E. J. (1997) Refinement of macromolecular structures by the maximum-likelihood method. *Acta Crystallogr., Sect. D: Biol. Crystallogr. 53*, 240−255.
(19) Emsley, P., and Cowtan, K. (2004) Coot: Model-building tools for molecular graphics. *Acta Crystallogr., Sect. D: Biol. Crystallogr. 60*, 2126−2132.
(20) Davis, I. W., Leaver-Fay, A., Chen, V. B., Block, J. N., Kapral, G. J., Wang, X., Murray, L. W., Arendall, W. B., 3rd, Snoeyink, J., Richardson, J. S., and Richardson, D. C. (2007) MolProbity: all-atom contacts and structure validation for proteins and nucleic acids. *Nucleic Acids Res. 35*, W375−383.
(21) Faeder, E. J., and Hammes, G. G. (1970) Kinetic studies of tryptophan synthetase. Interaction of substrates with the B subunit. *Biochemistry 9*, 4043−4049.
(22) Bar-Even, A., Noor, E., Savir, Y., Liebermeister, W., Davidi, D., Tawfik, D. S., and Milo, R. (2011) The moderately efficient enzyme: Evolutionary and physicochemical trends shaping enzyme parameters. *Biochemistry 50*, 4402−4410.
(23) Helgadottir, S., Rosas-Sandoval, G., Soll, D., and Graham, D. E. (2007) Biosynthesis of phosphoserine in the Methanococcales. *J. Bacteriol. 189*, 575−582.
(24) Mino, K., and Ishikawa, K. (2003) A novel O-phospho-L-serine sulfhydrylation reaction catalyzed by O-acetylserine sulfhydrylase from *Aeropyrum pernix* K1. *FEBS Lett. 551*, 133−138.
(25) Dunn, M. F., Aguilar, V., Brzovic, P., Drewe, W. F., Jr., Houben, K. F., Leja, C. A., and Roy, M. (1990) The tryptophan synthase bienzyme complex transfers indole between the α- and β-sites via a 25−30 Å long tunnel. *Biochemistry 29*, 8598−8607.
(26) Dunn, M. F., Niks, D., Ngo, H., Barends, T. R., and Schlichting, I. (2008) Tryptophan synthase: The workings of a channeling nanomachine. *Trends Biochem. Sci. 33*, 254−264.
(27) Burkhard, P., Tai, C. H., Ristroph, C. M., Cook, P. F., and Jansonius, J. N. (1999) Ligand binding induces a large conformational change in O-acetylserine sulfhydrylase from *Salmonella typhimurium*. *J. Mol. Biol. 291*, 941−953.
(28) Agren, D., Schnell, R., Oehlmann, W., Singh, M., and Schneider, G. (2008) Cysteine synthase (CysM) of *Mycobacterium tuberculosis* is an O-phosphoserine sulfhydrylase: Evidence for an alternative cysteine biosynthesis pathway in mycobacteria. *J. Biol. Chem. 283*, 31567−31574.
(29) Nakamura, T., Kawai, Y., Kunimoto, K., Iwasaki, Y., Nishii, K., Kataoka, M., and Ishikawa, K. (2012) Structural analysis of the substrate recognition mechanism in O-phosphoserine sulfhydrylase from the hyperthermophilic archaeon *Aeropyrum pernix* K1. *J. Mol. Biol. 422*, 33−44.
(30) Oda, Y., Mino, K., Ishikawa, K., and Ataka, M. (2005) Three-dimensional structure of a new enzyme, O-phosphoserine sulfhydrylase, involved in L-cysteine biosynthesis by a hyperthermophilic archaeon, *Aeropyrum pernix* K1, at 2.0A resolution. *J. Mol. Biol. 351*, 334−344.
(31) Sato, T., Fukui, T., Atomi, H., and Imanaka, T. (2003) Targeted gene disruption by homologous recombination in the hyperthermophilic archaeon *Thermococcus kodakaraensis* KOD1. *J. Bacteriol. 185*, 210−220.
(32) Sato, T., Fukui, T., Atomi, H., and Imanaka, T. (2005) Improved and versatile transformation system allowing multiple genetic manipulations of the hyperthermophilic archaeon *Thermococcus kodakaraensis*. *Appl. Environ. Microbiol. 71*, 3889−3899.
(33) Karr, E. A., Sandman, K., Lurz, R., and Reeve, J. N. (2008) TrpY regulation of trpB2 transcription in *Methanothermobacter thermautotrophicus*. *J. Bacteriol. 190*, 2637−2641.
(34) Hu, M., Zhang, C., Mu, Y., Shen, Q., and Feng, Y. (2010) Indole affects biofilm formation in bacteria. *Indian J. Microbiol. 50*, 362−368.
(35) Chant, E. L., and Summers, D. K. (2007) Indole signalling contributes to the stable maintenance of *Escherichia coli* multicopy plasmids. *Mol. Microbiol. 63*, 35−43.

(36) Chattoraj, D. K. (2007) Tryptophanase in sRNA control of the *Escherichia coli* cell cycle. *Mol. Microbiol. 63*, 1−3.
(37) Mueller, R. S., Beyhan, S., Saini, S. G., Yildiz, F. H., and Bartlett, D. H. (2009) Indole acts as an extracellular cue regulating gene expression in *Vibrio cholerae*. *J. Bacteriol. 191*, 3504−3516.
(38) Wang, D., Ding, X., and Rather, P. N. (2001) Indole can act as an extracellular signal in *Escherichia coli*. *J. Bacteriol. 183*, 4210−4216.
(39) Brzovic, P. S., Ngo, K., and Dunn, M. F. (1992) Allosteric interactions coordinate catalytic activity between successive metabolic enzymes in the tryptophan synthase bienzyme complex. *Biochemistry 31*, 3831−3839.
(40) Ferrari, D., Niks, D., Yang, L. H., Miles, E. W., and Dunn, M. F. (2003) Allosteric communication in the tryptophan synthase bienzyme complex: roles of the β-subunit aspartate 305-arginine 141 salt bridge. *Biochemistry 42*, 7807−7818.
(41) Ferrari, D., Yang, L. H., Miles, E. W., and Dunn, M. F. (2001) βD305A mutant of tryptophan synthase shows strongly perturbed allosteric regulation and substrate specificity. *Biochemistry 40*, 7421−7432.
(42) Jhee, K. H., McPhie, P., Ro, H. S., and Miles, E. W. (1998) Tryptophan synthase mutations that alter cofactor chemistry lead to mechanism-based inactivation. *Biochemistry 37*, 14591−14604.
(43) Rhee, S., Parris, K. D., Hyde, C. C., Ahmed, S. A., Miles, E. W., and Davies, D. R. (1997) Crystal structures of a mutant (βK87T) tryptophan synthase $\alpha_2\beta_2$ complex with ligands bound to the active sites of the α- and β-subunits reveal ligand-induced conformational changes. *Biochemistry 36*, 7664−7680.
(44) Yin, R., Frey, M., Gierl, A., and Glawischnig, E. (2010) Plants contain two distinct classes of functional tryptophan synthase beta proteins. *Phytochemistry 71*, 1667−1672.